Proc. Int. Conf. and Summer School on Advanced Silicide Technology 2014
JJAP Conf. Proc. **3** (2015) 011201

Band Structure Characterization of $K_8Ga_8Si_{38}$ Clathrates by Optical Measurement

Masaru Iioka[1], Haruhiko Udono[1]*, Motoharu Imai[2], and Masato Aoki[3]

[1]*Graduate school of Science and Engineering, Ibaraki University, Hitachi, Ibaraki 316-8511, Japan*
[2]*National Institute for Materials Science, Tsukuba, Ibaraki 305-0047, Japan*
[3]*Faculty of Engineering, Gifu University, Gifu 501-1193, Japan*

*E-mail: udono@mx.ibaraki.ac.jp

(Received July 17, 2014)

We have investigated the band structure of $K_8Ga_8Si_{38}$ clathrates by using optical reflectance measurements and first-principle calculations based on the density functional theory. The imaginary part of the dielectric function ε_2 was calculated from the normal reflectance spectrum via the Kramers-Kronig analysis. The experimental ε_2 values showed a fundamental absorption edge near 1 eV. From the analysis of the absorption spectrum, we found that the value of the absorption edge energy is approximately 1.2 eV for a $K_8Ga_8Si_{38}$ clathrate crystal.

1. Introduction

Group 14 clathrates consist of multiple X20, X24, and X28 polyhedral clusters that have cage-like frameworks of group 14 elements (host atoms), such as Si, Ge, and Sn, next to an encapsulated alkali or alkaline-earth metal that acts as a guest atom inside the structure [1]. Depending on the combination of the polyhedral clusters, two types of group 14 clathrate structures can be distinguished, which are denominated as type-I and type-II, whose chemical formulas are given by A_8X_{46} and $A_{24}X_{136}$, respectively, in which A represents the guest atom. Both types of clathrates have cubic crystal structures, and their space groups are Pm-3n and Fd-3m, for type-I and type-II clathrates, respectively [2]. In type-I clathrates, ternary clathrates exist in which part of the host atoms is substituted by group 13 elements, transition metals, and other elements [3].

Various studies on group 14 clathrates have been reported involving thermoelectric, superconducting, and semiconducting applications. Nolas et al. reported that the lattice thermal conductivity of the Ge-based ternary type-I clathrate $Sr_8Ga_{16}Ge_{30}$ is significantly reduced by rattling motion of encapsulated guest atoms [4]. Kawaji et al. determined the superconductivity of the Si-based type-I clathrate $(Na, Ba)_xSi_{46}$ [5]. Furthermore, based on electric structure calculations, Adams et al. demonstrated that Si clathrates Si_{46} and Si_{136}, also called the guest-free clathrates, are semiconductors with larger band gap energies than Si [6]. These reports reveal that the energy gap and electric structure of group 14 clathrates can be designed by combining host and guest elements.

From the viewpoint of material design, herein we have chosen for ternary type-I Si clathrates and investigated $K_8Ga_8Si_{38}$ as a novel solar cell material. In the previous study, it was found by first-principle calculations that $K_8Ga_8Si_{38}$ is an indirect band gap semiconductor with a gap energy of approximately 1.27 eV [7]. Previously, we reported the optical absorption spectrum of $K_8Ga_8Si_{38}$ by transmission measurements and observed an optical transmission below 0.4 eV. However, the value of the energy gap determined from the absorption spectrum is much smaller than the theoretical prediction. There are considerable reasons for this, one being the effect of dangling bond states created by vacancies in the cage-like framework, while another reason is the extrinsic absorption in the band gap associated with the high carrier density in $K_8Ga_8Si_{38}$ samples. In this

paper, we investigate the band structure of $K_8Ga_8Si_{38}$ by normal reflectance measurement and compare the experimental spectra with theoretical ones, the latter being based on first-principle calculations.

2. Experimental procedures

Bulk single crystalline $K_8Ga_8Si_{38}$ was synthesized by a reaction of K, Ga, and Si [8]. The elements of the stoichiometric mixture were sealed in a Ta capsule under an Ar atmosphere. The capsule was heated up to 1270K for 3 h and annealed at 970K for 60 h, after which it was naturally cooled down to room temperature. The polyhedrally shaped grown crystals had mirror-like growth facets. For optical transmittance (*T*) and reflectance (*R*) measurements, plate-like samples were prepared by a grinding and polishing process using Al_2O_3 powder and fumed silica. The thickness of the samples was less than 40 μm and 1000 μm for transmittance and reflectance measurements, respectively.

The optical transmittance and reflectance measurements were carried out at room temperature using a microscopic FT-IR system (800-8000 cm^{-1}) and NIR-VIS microspectroscopy (4600-25000 cm^{-1}), respectively [9]. The refractive index (*n*) and extinction coefficient (*k*) were calculated from the normal reflectance spectrum via the modified Kramers-Kronig analysis [10]. The dielectric function, $\varepsilon = \varepsilon_1 - i\varepsilon_2$, was obtained from the *n* and *k* values via Eq. (1).

$$\varepsilon_1 = n^2 - k^2, \quad \varepsilon_2 = 2nk \tag{1}$$

The optical absorption coefficient α was derived from both the transmittance and reflectance spectrum using Eqs. (2) and (3) :

$$T = \{(1-R)^2 \exp(-\alpha d)\}/\{1 - R^2 \exp(-2\alpha d)\} \tag{2}$$

$$\alpha = 4\pi k/\lambda \tag{3}$$

where *d* is the sample thickness and λ is the wavelength.

The electronic structure was calculated based on the density functional theory using the VASP5.2 software with the projector-augmented (PAW) method and a PBE-type exchange-correlation energy functional [11, 12]. The lattice parameter and atomic position were defined according to previous literature [13]. The theoretical complex dielectric functions in the long wavelength limit (*i.e.* $\mathbf{q} \rightarrow 0$), specified by $\varepsilon_{ii}(\omega)$ in which *i* and ω respectively denote the Cartesian axis in which the Bloch vector **q** of the incident wave is pointing and the angular frequency, were calculated within the PAW and Kohn-Sham framework [14], using their implementation in the VASP package. Theoretical optical absorption coefficients were then calculated through Eqs. (1) and (3) using the calculated complex dielectric functions.

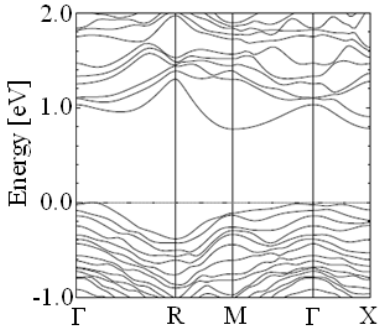

Fig. 1 The calculated band structure of simple cubic $K_8Ga_8Si_{38}$. Energies (i.e. Kohn-Sham eigenvalues) are measured from the top of the valence band.

3. Results and discussion

Figure 1 shows the calculated electric structure of the $K_8Ga_8Si_{38}$ crystal. The valence band maximum (VBM) is located along the lines defined by Γ, whereas the conduction band minimum (CBM) is located along the *X* and *M* lines. This geometric description coincides with a previous study, in which this was calculated via CASTEP [7]. The energy gap (E_g) between the VBM and CBM is 0.80 eV, which is approximately 0.15 eV higher than the calculated E_g of Si. This result is consistent with previous calculations [7, 8].

Figure 2(a) shows the experimental non-polarized reflectance spectrum and theoretical reflectance spectrum of $K_8Ga_8Si_{38}$. In the theoretical reflectance spectrum, no significant optical reflectance anisotropy is found, since $K_8Ga_8Si_{38}$ has a cubic crystal structure. The experimental reflectance was about 32% for a photon energy of 1.0 eV, and increased monotonically up to about 53%, corresponding to a photon energy of 3 eV. This behavior is similar to the theoretical prediction. The refractive index *n* and extinction coefficient *k* for both experimental and theoretical data are plotted in Fig. 2(b). The experimental refractive indices of $K_8Ga_8Si_{38}$, given by $n = 3.6$ at 1 eV and $n = 3.5$ at 0.7 eV, are slightly higher when compared to those of bulk Si ($n = 3.50$ at 1 eV and $n = 3.46$ at 0.7 eV) [15].

A comparison of the imaginary part of complex dielectric function between the experimental data, which was calculated via the Kramers-Kronig analysis, and the theoretical data of $K_8Ga_8Si_{38}$ is shown in Fig. 3(a). The fundamental absorption edge near 1 eV for the experimental data was higher than the one observed in the theoretical data, even though the theoretical calculation is based on a temperature of 0K. This discrepancy in the lower energy range is frequently observed in the theoretical spectrum mainly due to a limited energy resolution in the calculation. The plot of $\alpha^{1/2}$, which was derived from the experimental optical reflectance, versus the photon energy hν near the absorption edge is presented in Fig. 3(b). The absorption edge energy determined from extrapolating $\alpha^{1/2}$ to a value of zero was approximately 1.2 eV, which is approximately 0.08 eV larger than E_g value of Si. This result is consistent with the present and previous calculated results [7, 8] for which the E_g of $K_8Ga_8Si_{38}$ was determined to be approximately 0.1-0.15 eV larger than E_g of Si [8].

Optical transmission between photon energies given by 0.2 eV and 0.4 eV was found for several thin $K_8Ga_8Si_{38}$ samples. However, both the limited transmission width in the photon energy and the high absorption coefficient across the spectrum would suggest the influence of extrinsic absorption

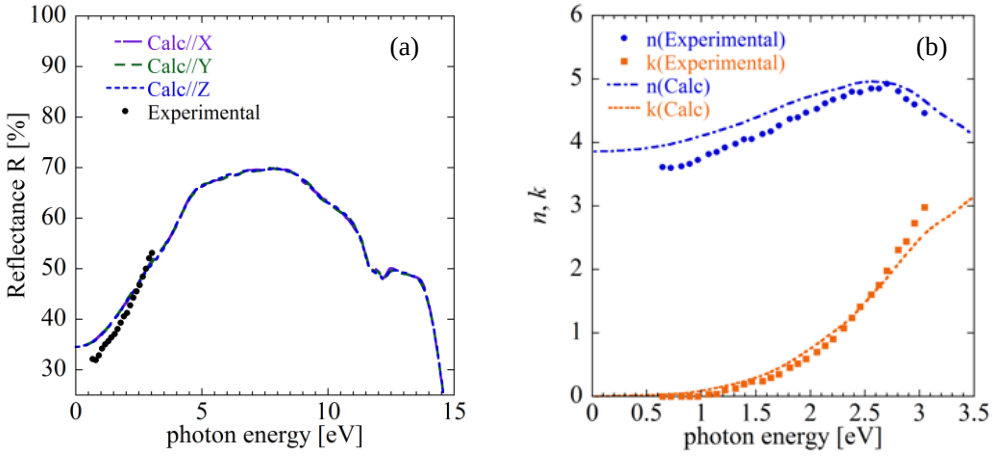

Fig. 2 (a) Optical reflectance spectra of single crystalline $K_8Ga_8Si_{38}$. The dotted and dashed lines indicate experimental data measured under normal optical incidence and calculated data for incident directions along the X, Y, and Z axes, respectively. (b) Refractive index *n* and extinction coefficient *k*. The dotted and dashed lines represent experimental and calculated data, respectively.

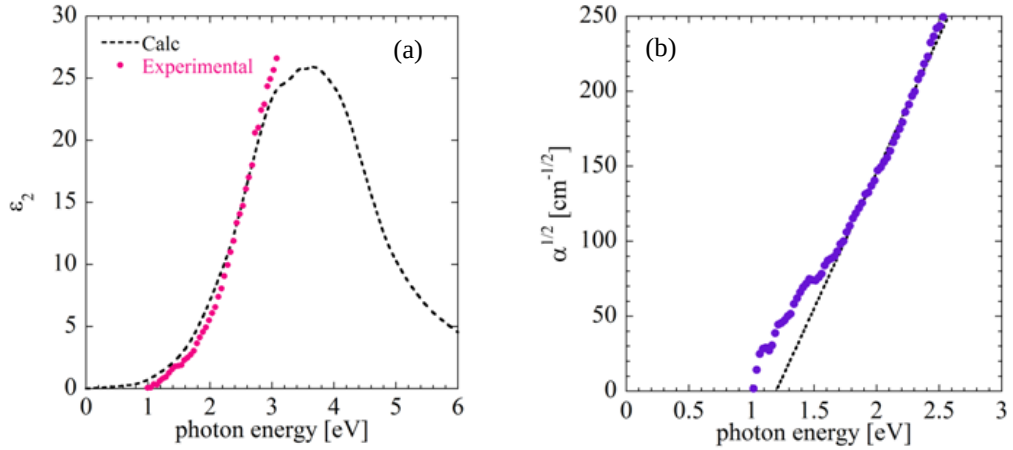

Fig. 3 (a) Imaginary part of the dielectric function ε_2. The dotted and dashed lines indicate experimental calculated data. (b) Plot of $\alpha^{1/2}$ vs. the photon energy.

such as free carrier absorption, impurity band absorption, and crystal disorder absorption below the energy gap, which is attributed to the high carrier density in the samples [8]. Thus, we can conclude that the absorption edge energy derived from the reflectance spectrum is the fundamental energy gap of the $K_8Ga_8Si_{38}$ clathrate crystal.

4. Conclusions

We investigated the absorption edge energy of single crystalline $K_8Ga_8Si_{38}$ clathrates by optical transmittance and reflectance measurements. From the optical absorption spectrum, which is calculated based on the normal reflectance spectrum, we found that the fundamental absorption edge of $K_8Ga_8Si_{38}$ is approximately 1.2 eV at room temperature.

Acknowledgment

This research was partially supported by a grant from the Advanced Low Carbon Technology Research and Development Program (ALCA) of the Japan Science and Technology Agency (JST).

References

[1] J. S. Kasper, P. Hagenmuller, M. Pouchard and C. Cros, Science **150** (1965) 1713.
[2] K. A. Kovnir and A. V. Shevelkov, Russ. Chem. Rev. **73** (2004) 923.
[3] S. Bobev and S. C. Sevov, J. Solid State Chem. **153** (2000) 92.
[4] G. S. Nolas, J. L. Cohn, G. A. Slack, and S. B. Schujman Appl. Phys. Lett. **73** (1998) 178.
[5] H. Kawaji, H. Horie, S. Yamanaka, and M. Ishikawa, Phys. Rev. Lett. **74** (1995) 1427.
[6] G. B. Adams, M. O'Keeffe, A. A. Demkov, O. F. Sankey, and Y. M. Huang, Phys. Rev. B **49** (1994) 8048.
[7] Y. Imai and M. Imai, J. Alloys Compd. **509** (2011) 3924.
[8] M. Imai, A. Sato, H. Udono, Y. Imai, and H. Tajima, Dalton Trans. **40** (2011) 4045.
[9] H. Udono, I. Kikuma, H. Tajima, and K. Takarabe, J. Mater. Sci.: Mater. Electron **18** (2007) 65.
[10] R. K. Ahrenkiel, J. Opt. Soc. Am. **61** (1971) 1651.
[11] G. Kresse and J. Furthmüller, Comput. Mater. Sci. **6** (1996) 15.
[12] P. E. Blöchl, Phys. Rev. B **50** (1994) 17953.
[13] R. Kröner, K. Peters, H. G. von Schnering, and R. Nesper, Z. Krist. NSC **213** (1998) 667.
[14] M. Gajdoš, K. Hummer, G. Kresse, J. Furthmüller, and F. Bechstedt, Phys. Rev. B **73** (2006) 045112.
[15] H. W. Verleur, J. Opt. Soc. Am. **10** (1968) 1356.